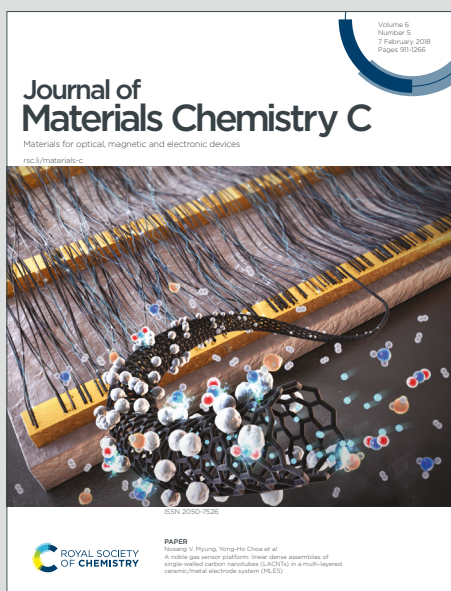


# Journal of Materials Chemistry C

Materials for optical, magnetic and electronic devices

Accepted Manuscript

This article can be cited before page numbers have been issued, to do this please use: L. Zhang, Z. Yan, Z. Tu, Z. Wu and Y. Zheng, *J. Mater. Chem. C*, 2019, DOI: 10.1039/C9TC03937F.



This is an Accepted Manuscript, which has been through the Royal Society of Chemistry peer review process and has been accepted for publication.

Accepted Manuscripts are published online shortly after acceptance, before technical editing, formatting and proof reading. Using this free service, authors can make their results available to the community, in citable form, before we publish the edited article. We will replace this Accepted Manuscript with the edited and formatted Advance Article as soon as it is available.

You can find more information about Accepted Manuscripts in the [Information for Authors](#).

Please note that technical editing may introduce minor changes to the text and/or graphics, which may alter content. The journal's standard [Terms & Conditions](#) and the [Ethical guidelines](#) still apply. In no event shall the Royal Society of Chemistry be held responsible for any errors or omissions in this Accepted Manuscript or any consequences arising from the use of any information it contains.

## ARTICLE

Cite this: DOI:

Received 00th January 2019,  
Accepted 00th January 2019

DOI:

www.rsc.org/

**Green-emitting iridium(III) complexes containing pyridine sulfonic acid as ancillary ligands for efficient OLEDs with extremely low efficiency roll-off**Lin Zhang,<sup>1</sup> Zhi-Ping Yan,<sup>1</sup> Zhen-Long Tu,<sup>1</sup> Zheng-Guang Wu,<sup>1</sup> You-Xuan Zheng<sup>1,2\*</sup>

A novel ancillary ligand of pyridine sulfonic acid (PySO<sub>3</sub>) was developed for two green-emitting iridium(III) compounds, Ir1 ( $\lambda_{\text{max}} = 496$  nm) and Ir2 ( $\lambda_{\text{max}} = 504$  nm), with trifluoromethyl-substituted 2-phenylpyridine derivatives as main ligands. Due to the strong electron-withdrawing ability of PySO<sub>3</sub>, both complexes have relatively low LUMO energy levels and good electron mobility, which benefit the charge balance in the organic light-emitting diodes (OLEDs) during the electroluminescence process. Therefore, all devices with double light-emitting layers exhibit good performances. Particularly, device using Ir2 as emitter obtains a maximum luminance above 92000 cd m<sup>-2</sup>, a maximum external quantum efficiency (EQE<sub>max</sub>) of 25.5% with an extremely low efficiency roll-off, as well as the EQE still remains 22.9% at the high luminance of 20000 cd m<sup>-2</sup>. These results demonstrate that pyridine sulfonic acid is a potential and charming ligand for Ir(III) complexes and high-performance OLEDs.

**Introduction**

As a new-generation technology in flat-panel display, organic light-emitting diode (OLED) has basked in the limelight, due to its high brightness, fresh color and the potential in flexible display.<sup>1-8</sup> Among the various emitting materials utilized in OLEDs, iridium(III) complexes are prominent due to the variable ligand structure and tunable emission color. Moreover, the heavy iridium atoms lead to strong spin-orbit coupling, allowing Ir(III) complexes to capture both singlet and triplet excitons for light emission with theoretically 100% internal quantum efficiency (IQE).<sup>3,9</sup>

However, the efficiency roll-off is serious at high luminance for most efficient OLEDs based on Ir(III) emitters, which is mainly due to the unbalanced electron-hole injection, transport, combination and some nonradioactive processes.<sup>10</sup> Particularly, the electron-hole balance in emissive layer is one of the most important factors for achieving high-performance OLEDs. Generally, using bipolar host materials and high electron transport property dopant are two main methods to achieve electron-hole balance in OLEDs.<sup>11,12</sup> Owing to the excellent performance of commercially available bipolar host material 2,6-bis-(3-(carbazol-9-yl)phenyl)pyridine (2,6-DCzPPy) in practical applications, it is highly desirable to develop new kinds of Ir(III) complexes to achieve effective devices with low efficiency roll-off ratios.

At the same time, several Ir(III) complexes with sulfonyl group in the main ligands have been reported and exhibited unique advantages for OLEDs.<sup>13-19</sup> According to the special structure of

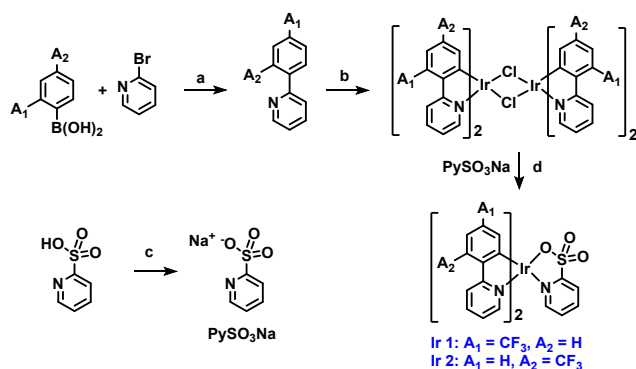
sulfonyl groups, it would show potential application in furnishing electron injection (EI) and electron transporting (ET), which is further used to promote the electroluminescence (EL) performance. For example, Zhou et al. introduced phenylsulfonyl substituent into the main ligands of the Ir(III) compound, and proved that the SO<sub>2</sub>Ph group can improve the EI/ET ability of the complexes, which show good device performances with a maximum external efficiency (EQE<sub>max</sub>) of 10.67%, a maximum luminance ( $L_{\text{max}}$ ) of 48567 cd m<sup>-2</sup> as well as a relatively low efficiency-off with the EQE of 8.90% at the luminance of 6000 cd m<sup>-2</sup>.<sup>16</sup> Wong and co-workers introduced aromatic sulfonyl groups with different fluorine substituents into Ir(III) complexes showing excellent EL performances afford by their EI/ET abilities.<sup>19</sup> All these results sufficiently indicate that sulfonyl groups take advantages in electron-hole balance. As a result, it is necessary to further study more Ir(III) complexes containing sulfonyl groups for efficient OLEDs with low efficiency roll-off.

As is well known, pyridine sulfonic acid not only has similar characteristics as SO<sub>2</sub>Ph group but also possess the advantages of simple structure and easy synthesis. However, current research fields on pyridine sulfonic acids as ligands are limited, and most of them concern about oxidation catalysis,<sup>20,21</sup> anticancer metallodrugs<sup>22</sup> and supramolecular framework.<sup>23,24</sup> The researches on phosphorescent Ir(III) complexes containing pyridine sulfonic acid for OLEDs are rare. Herein, two green-emitting complexes with 2-(4-(trifluoromethyl)phenyl)pyridine (4-tfppy) or 2-(2-(trifluoromethyl)phenyl)pyridine (2-tfppy) as main ligands and pyridine sulfonic acid (PySO<sub>3</sub>) as ancillary

ligand were investigated. Compared with other ancillary ligands, the strong electron-withdrawing  $\text{PySO}_3$  group reduces the LUMO energy levels of the complexes apparently and enhances their electron mobility, which would improve their EI/ET properties and finally maintain the balance of charge transport during the EL process. Hence, the OLEDs exhibit excellent performances with a  $L_{\text{max}}$  of  $92297 \text{ cd m}^{-2}$  and an  $\text{EQE}_{\text{max}}$  of 25.5%. Notably, at the luminance of  $10000 \text{ cd m}^{-2}$  and  $20000 \text{ cd m}^{-2}$ , the EQE still remains as 24.5% and 22.9%, respectively, indicating an extremely low efficiency roll-off.

## Results and discussion

### Synthesis and characterization



(a)  $\text{Pd}(\text{PPh}_3)_4$ ,  $\text{Na}_2\text{CO}_3$ ,  $\text{THF}/\text{H}_2\text{O}$ ,  $80^\circ\text{C}$ , 10 h; (b)  $\text{IrCl}_3$ ,  $\text{C}_2\text{H}_5\text{OCH}_2\text{CH}_2\text{OH}$ ,  $115^\circ\text{C}$ , 12 h; (c)  $\text{NaOH}$ ,  $\text{CH}_3\text{OH}/\text{C}_2\text{H}_5\text{OC}_2\text{H}_5$ ; (d)  $\text{PySO}_3\text{Na}$ ,  $\text{C}_2\text{H}_5\text{OCH}_2\text{CH}_2\text{OH}$ ,  $110^\circ\text{C}$ , 8 h.

**Scheme 1** Synthetic route of Ir(III) complexes.

The chemical structures and synthetic methods of the compounds are shown in Scheme 1. The main ligands were synthesized using traditional Suzuki coupling reactions, and the complexes were prepared by common methods with good yields (see supporting information for details). Gradient sublimation method was carried out for further refinement. The resulting complexes were fully characterized by  $^1\text{H}$  NMR,  $^{13}\text{C}$  NMR,  $^{19}\text{F}$  NMR and high resolution electrospray ionization mass spectroscopy (HR ESI-MS).

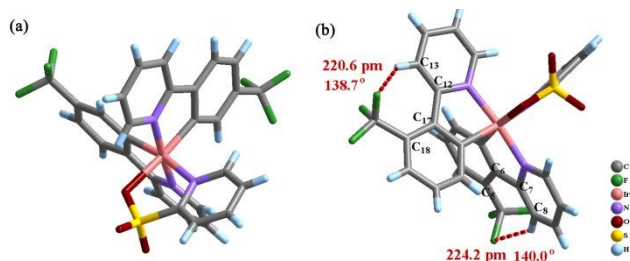


**Fig. 1** X-ray crystal structure of (a) Ir1 (CCDC: 1936819) and (b) Ir2 (CCDC:1937037).

Single crystal diffraction analysis was utilized to confirm the molecular structures of Ir1 and Ir2 (Fig.1, Fig.S4), and their detailed data are available in Table S1-S2. The bond lengths between Ir(III) atoms and  $\text{PySO}_3$  ligands are  $2.20 \text{ \AA}$  and  $2.17 \text{ \AA}$

for Ir-O and Ir-N, respectively, which are slightly longer than the reported bond lengths of  $2.15 \text{ \AA}$  for analogous complexes with pyridine carboxylate (pic) as ancillary ligands.<sup>25</sup> The longer bond lengths resulting from strong polarity of  $\text{S}=\text{O}$  bonds indicate the slighter weaker coordination ability of  $\text{PySO}_3$ , which conforms to the reported results as well. **Error! Bookmark not defined.** The rest of Ir-N and Ir-C bond lengths range from  $1.98\text{-}2.01 \text{ \AA}$  and  $2.03\text{-}2.04 \text{ \AA}$ , respectively, which are in agreement with other reported complexes.<sup>13,26</sup> It is noticeable that the trifluoromethyl group on the position 2 of phenyl ring causes more deformation of main ligand because of the repulsion between the trifluoromethyl group and pyridine ring. As the crystal data proves, the torsion angles of  $\text{C}_5\text{-C}_6\text{-C}_7\text{-C}_8$  and  $\text{C}_{13}\text{-C}_{12}\text{-C}_{17}\text{-C}_{18}$  in complex Ir2 are  $-9.3^\circ$  and  $1.5^\circ$ , respectively, which is larger than torsion angle in Ir1 ( $7.1^\circ$ ,  $0.5^\circ$ ). Besides, the trifluoromethyl group in Ir2 may induce the  $\text{C-H}\cdots\text{F}$  H-bond with the H atom on position 3 of pyridine ring. According to the crystal structure of Ir2, the  $\text{C-H}\cdots\text{F}$  angles are in the range of  $138.7^\circ\text{-}140.0^\circ$  with  $\text{H}\cdots\text{F}$  distances of  $2.21\text{-}2.24 \text{ \AA}$ , which satisfies the IUPAC criteria for the hydrogen bond and would limit the trifluoromethyl group rotation, molecular vibration and improve the luminescence intensity.<sup>27-29</sup>

The decomposition temperature ( $T_d$ ) of the complexes should be high enough to avoid decomposition during the operation of the OLEDs. Therefore, the thermal stability of Ir1 and Ir2 were investigated through thermogravimetric analysis (TGA), which gives  $T_d$  as  $384^\circ\text{C}$  and  $376^\circ\text{C}$ , respectively (Fig. S7). Although the coordination ability of  $\text{PySO}_3$  is slightly weaker than pyridine carboxylate as mentioned, the thermal stability of complexes still meets the requirement.

### Photophysical property

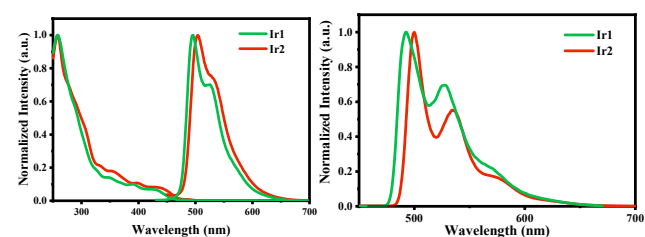


**Fig.2** (a) UV-Vis absorption and emission spectra of the complexes in  $\text{CH}_2\text{Cl}_2$  at 298 K and (b) emission spectra in  $\text{CH}_2\text{Cl}_2$  at 77 K.

The UV-Vis absorption and photoluminescence (PL) spectra of Ir1 and Ir2 at room temperature are shown in Fig.2, and their PL spectra in dichloromethane at 77 K are included as well. The relevant data are listed in Table 1. The UV-Vis absorption spectra of two complexes can be divided into three parts. The strongest absorption peak under  $320 \text{ nm}$  comes from the spin-allowed  $\pi\text{-}\pi^*$  transition of the ligands. From  $320$  to  $410 \text{ nm}$ , the absorption peaks become weaker and can be attributed to the spin-allowed metal-ligand charge transfer ( $^1\text{MLCT}$ ), while the weakest  $^3\text{MLCT}$  bands located between  $410$  and  $470 \text{ nm}$ .

Complexes Ir1 and Ir2 exhibit maximum emission peaks at 496 and 504 nm, which are in the green region with CIE coordinates at (0.22, 0.59) and (0.24, 0.58), respectively. Compared with the complexes using same main ligands and common ancillary ligands, such as acetylacetonate (acac)<sup>30</sup> or tetraphenylimidodiphosphinate (tpip)<sup>31</sup>, Ir1 exhibit a blue shift of near 30 nm resulting from the impact of PySO<sub>3</sub> group on the electron cloud distribution of the complex. The position of the trifluoromethyl group on the phenyl ring also affects the

photophysical property of the complexes slightly, as the emission spectrum of Ir2 is redshifted than that of Ir1. At 77 K in the frozen solutions, the PL spectra of both complexes are blue shifted and highly structured (Fig. 2(b)), which may due to the increasing of the triplet ligand-centered transition (<sup>3</sup>LC).<sup>32</sup> The triplet energy levels (*T*<sub>1</sub>) of Ir1 and Ir2 are 2.63 and 2.59 eV, respectively, and the low-lying *T*<sub>1</sub> could enhance energy transfer between the hosts and emitters as well.

**Table 1.** Photophysical and electrochemical properties of Ir1 and Ir2.

complex	<i>T</i> <sub>d</sub> <sup>a</sup> (°C)	$\lambda_{abs}$ <sup>b</sup> (nm)	$\lambda_{em}$ <sup>b</sup> (nm)	$\lambda_{em}$ <sup>c</sup> (nm)	CIE <sup>b</sup> (x, y)	$\tau$ <sup>b</sup> ( $\mu$ s)	$\Phi$ <sup>d</sup> (%)	HOMO/LUMO <sup>e</sup> (eV)
Ir1	384	258, 390	496, 525	493, 528	(0.22, 0.59)	1.45	41.84%	(-5.79, -3.28)
Ir2	376	258, 395	504, 529	500, 534	(0.24, 0.58)	1.66	69.64%	(-5.78, -3.36)

<sup>a</sup>) Decomposition temperature; <sup>b</sup>) Measured in degassed CH<sub>2</sub>Cl<sub>2</sub> solution ( $5 \times 10^{-5}$  mol L<sup>-1</sup>) at room temperature; <sup>c</sup>) Measured in degassed CH<sub>2</sub>Cl<sub>2</sub> solution ( $5 \times 10^{-5}$  mol L<sup>-1</sup>) at 77 K; <sup>d</sup>) Absolute PLQY in co-deposited films with 2,6-DCzPPy; <sup>e</sup>) From the oxidation potentials of the cyclic voltammetry (CV) diagram using ferrocene as the internal standard and the band gap from the absorption spectra in degassed solution. HOMO (eV) =  $-(E_{ox}-E_{1/2,Fe})-4.8$ , LUMO(eV)=HOMO+*E*<sub>bandgap</sub>.

The absolute photoluminescence quantum yields (PLQY) of two complexes in CH<sub>2</sub>Cl<sub>2</sub> and doped films were measured (Fig. S5-S6, Table S4). Due to the strong interaction between the complexes and solvent molecules, the vibrating movement of the complexes is violent leading to a large non-radiative constant (*k*<sub>nr</sub>) and undesired PLQYs in CH<sub>2</sub>Cl<sub>2</sub> solution (3.50% for Ir1 and 5.87% for Ir2, respectively). However, in the co-deposited films with widely used OLED host materials of 2,6-DCzPPy or 4,4',4''-tri(9-carbazoyl)triphenylamine (TCTA), the PLQYs become much higher. The PLQYs of Ir1 and Ir2 in co-deposited films with 2,6-DCzPPy are up to 41.84% and 69.64% respectively, while in doped films with TCTA, the PLQYs still exceed 40%. In most cases, the photophysical properties of emitters in doped films can better reflect the actual properties of devices, therefore, it has important reference values for exploring its device performances.<sup>33</sup> Furthermore, the phosphorescence lifetimes ( $\tau$ ) of Ir1 and Ir2 are 1.45 and 1.66  $\mu$ s in CH<sub>2</sub>Cl<sub>2</sub>, respectively, which are short enough to avoid severe triplet-triplet annihilation (TTA) of the OLEDs.

### Electrochemistry and theoretical calculation

The cyclic voltammetry (CV) is a common method to estimate the energy levels of the complexes, and for reversible oxidation-reduction potential the results are credible.<sup>34</sup> The highest occupied molecular orbital (HOMO) and lowest unoccupied molecular orbital (LUMO) energy levels of these complexes were calculated through redox potential data (Fig. S8, Table 1) and the bandgaps (*E*<sub>g</sub>) were derived from the UV-Vis spectra. During the anodic scan, two complexes exhibit reversible redox peaks at 1.0 and 1.1 V, respectively, which belong to the metal-centered Ir<sup>3+</sup>/Ir<sup>4+</sup> redox pairs. The position of trifluoromethyl group has little effect on redox process, as the oxidation peaks

of Ir1 and Ir2 are nearly the same, leading to the similar HOMO energy levels (-5.79 and -5.78 eV, respectively). Due to the longer UV cut-off wavelength of Ir2, the complex obtains slightly lower LUMO energy level (-3.36 eV) than that of Ir1 (-3.28 eV). Deserved to be mentioned, the strong electron-withdrawing PySO<sub>3</sub> shifts the HOMO/LUMO energy levels of the complexes downwards distinctly. According to reported complexes with acac or tpip as ancillary ligands,<sup>33,34</sup> the LUMO level of Ir1 reduced by about 0.25 eV, which would be beneficial for high electron mobility of two complexes.

**Table 2** Theoretical calculation data of orbital distributions.

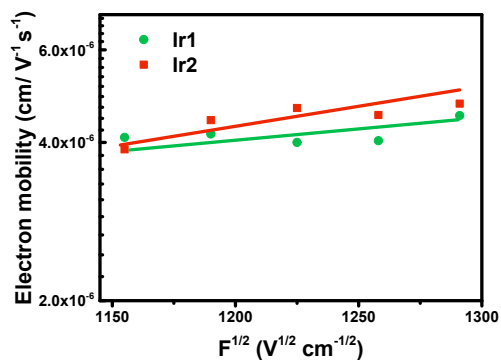
Complex	Orbital	Calculated Energy levels / eV	Composition (%)		
			Ir atom	Main Ligands	Ancillary ligand
Ir1	HOMO-2	-6.51	39.10	57.22	3.68
	HOMO-1	-6.36	26.23	62.62	11.16
	HOMO	-5.74	44.41	51.69	3.90
	LUMO	-1.95	93.12	4.17	2.71
	LUMO+1	-1.84	81.03	4.94	14.03
	LUMO+2	-1.73	14.19	3.26	82.55
Ir2	HOMO-2	-6.49	49.96	46.49	3.55
	HOMO-1	-6.37	65.83	20.02	14.15
	HOMO	-5.71	51.56	44.78	3.66
	LUMO	-1.97	4.41	92.74	2.84
	LUMO+1	-1.88	4.62	92.97	2.42
	LUMO+2	-1.73	3.19	3.34	93.38

Theoretical calculations were also carried out through time-dependent density function theory (TD-DFT), and B3LYP with 6-31G (d, p) and LanL2DZ basis sets to obtain deep insight into the orbital distributions of two complexes. The conductor-like polarizable continuum model (C-PCM) method was carried out

to calculate the solvent effect of  $\text{CH}_2\text{Cl}_2$ . The orbital distribution data of several molecular orbitals (MOs) are listed in Table 2, and their optimized structures and electron cloud distributions are shown in Fig. S10. For most Ir(III) complexes, the main ligands and Ir atom greatly affect the photophysical properties of the complexes as the HOMO/LUMO levels mainly situate on them. And the effects of ancillary ligands on electron cloud distribution are significant as well (2.71%-93.38%), which leads to the unusual HOMO/LUMO energy levels and the blueshift of emission spectra.

### Electron mobility

As the hole mobility of the hole transport materials are much higher than the electron mobility of the electron transport materials, the electron mobility of the dopant materials cause great impact on the charge balance and affect the efficiency and efficiency roll-off of the OLEDs greatly.<sup>35,36</sup> Thus, emitters with good electron mobility could benefit the transportation of the electron leading to a more balanced distribution of hole/electron



and suppressing the annihilation of excitons, which helps to promote the device performances.<sup>37</sup>

**Fig. 3** Electron mobility of the complexes as a function of the square of the electric field.

The transient electroluminescence (TEL) method is a convenient and efficient method to measure the transport mobility of the materials.<sup>38</sup> Therefore, it was carried out to estimate the electron mobility of the complexes based on device structures of ITO/ TAPC ((*bis*(4-(*N,N*-ditolylamino)phenyl)cyclohexane, 60 nm)/ Ir(III) complexes (60 nm)/ LiF (1 nm)/ Al (100 nm). (Fig. S11) In which the TAPC acts as hole transport layer, while the complexes act as emission/electron transport layer. And the calculated electron mobility of Ir1 and Ir2 are in the range of 4.00 - 4.50 × 10<sup>-6</sup> and 3.88 - 4.74 × 10<sup>-6</sup> cm<sup>2</sup> V<sup>-1</sup> s<sup>-1</sup> (Fig. 3), respectively, which are comparable to that of the electron mobility of traditional electron transport material Alq<sub>3</sub> (tris(8-hydroxyquinolinato)aluminum, 3.65 - 4.21 × 10<sup>-6</sup> cm<sup>2</sup> V<sup>-1</sup> s<sup>-1</sup>, Fig. S12). The aromatic sulfonyl groups, as an electron-withdrawing group without extended  $\pi$  conjugation, has been used in many ligands to improve the electron mobility of the complexes.<sup>13,17,19</sup> Therefore, PySO<sub>3</sub> which retains the structural

character of the phenylsulfonyl group (S=O) could contribute to the good electron mobility of two complexes as well, and finally promote their device performances.

### OLED performance

Devices D1 and D2 using Ir1 and Ir2 as emitters, respectively, were fabricated to evaluate the EL performances with the configuration of ITO/ HAT-CN (hexazatriphenylenehexacarbonitrile, 6 nm)/ TAPC (60 nm)/ TCTA (10 nm): Ir(III) complexes (8 wt%)/ 2,6-DCzPPy (10 nm): Ir(III) complexes (8 wt%)/ TmPyPB (1,3,5-*tri*((3-pyridyl)-phen-3-yl)benzene, 60 nm)/ LiF (1 nm)/ Al (100 nm). HAT-CN and LiF were employed as interface modified materials for anode and cathode, respectively. TAPC which has good hole mobility and high LUMO level acted as hole-transport/electron-block layer, and TCTA/2,6-DCzPPy were used as host materials, while TmPyPB served as electron-transport/hole-block layer due to its high electron mobility and low HOMO level.<sup>39-41</sup> The energy level diagram of the devices and chemical structures of the relevant materials are listed in Fig. 4. The device performances are shown in Fig. 5, including EL spectra, current efficiency ( $\eta_c$ ) and external quantum efficiency (EQE) verse luminance ( $L$ ) curves. The corresponding key data are listed in Table 3, and other EL performances data can be found in Fig. S11.

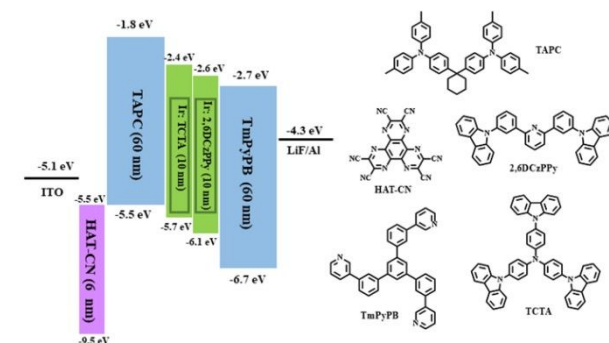


**Fig. 4** The device structure and the energy level diagram of the HOMO and LUMO levels of materials employed in this work and their chemical structures.

Devices D1 and D2 exhibit green emissions with maximum peaks at 496 and 507 nm with CIE coordinates of (0.22, 0.59) and (0.24, 0.64), respectively, which are similar to their PL spectra in solution indicating that the EL emission mainly comes from the triplet excited states of the emitters. And there are no residue emissions of host materials around 400 nm, implying that the energy completely and effectively transfers from the host to the complexes under the electric excitation.

Both devices exhibit pretty well performances. For device D1, a  $L_{\text{max}}$  of 44885 cd m<sup>-2</sup>, a maximum current efficiency ( $\eta_{c, \text{max}}$ ) of 69.7 cd A<sup>-1</sup>, an EQE<sub>max</sub> of 21.7% and a maximum power efficiency ( $\eta_{p, \text{max}}$ ) of 41.8 lm W<sup>-1</sup> are obtained. And device D2 exhibits better EL performances with a  $L_{\text{max}}$  of 92297 cd m<sup>-2</sup>, a

$\eta_{c,max}$  of 91.4  $\text{cd A}^{-1}$ , an  $\text{EQE}_{max}$  of 25.5% and a  $\eta_{p,max}$  of 59.5  $\text{lm W}^{-1}$ , respectively. As the emitters exhibit similar emission spectra and electron mobility, the differences in the EL performances mainly origin from the higher PLQY and lower LUMO energy levels of Ir2, which benefited the electron injection process and contributed to the charge balance of the device D2. Moreover, for Ir2 in doped films, there might be intramolecular hydrogen bond similar to the observation in crystal structure, which could limit the rotation of the trifluoromethyl group and molecular vibration, and slightly alleviate the non-radiative transition process and benefit its EL performances ultimately.

According to the recent reports, green-emitting OLEDs whose  $\text{EQE}_{max}$  mainly located in the range of 16.6%-28.7% always obtain sharply declined  $\text{EQE-L}$  curves at the high luminance.<sup>42-47</sup> For example, Tong et al. reported a green-emitting device with the  $\text{EQE}_{max}$  of 25.2%, the  $L_{max}$  of 27450  $\text{cd m}^{-2}$  and the efficiency roll-off ratio reached 9.5% at the luminance of 1000  $\text{cd m}^{-2}$ .<sup>43</sup> Chen and coworkers fabricated high performance devices with the lowest efficiency roll-off value of 7.9% at the 10000  $\text{cd m}^{-2}$  among the selected literatures, but the efficiency is less impressive with the  $\text{EQE}_{max}$  of 20.0%.<sup>44</sup> The devices in this case possess good efficiency and extremely low efficiency roll-off with flat  $\text{EQE-L}$  curves (Fig. 5(b)). At the high luminance of 10000  $\text{cd m}^{-2}$ , the  $\text{EQE}$  of

device D1 can be kept at 20.5% with a small efficiency roll-off ratio of 5.5% compared with the  $\text{EQE}_{max}$ . And this characteristic becomes more outstanding for device D2, as the EQEs still maintain at 24.5% and 22.9% when the luminance reach at 10000 and 20000  $\text{cd m}^{-2}$ , respectively, which only decrease by 3.2% and 9.5%. In theory, the good device performances can be explained by the balanced electron-hole transportation and subdued nonradiative quenching processes. Firstly, the double light-emitting layers can widen the excitons recombination zone efficiently, which alleviate the excitons annihilation resulting from the high density of the excitons at the interface of the organic layers.<sup>48</sup> Secondly, the HOMO energy gap between TAPC and 2,6-DCzPPy could be reduced because of another emitting layer TCTA, which decreases the hole injection barrier efficiently and finally promotes the device performances. Thirdly, the emitters have their own superiority. The lifetimes of the emitters are short enough to avoid serious triplet-triplet annihilation and the bulky trifluoromethyl substituents in the main ligands may increase the molecular distance which alleviate the self-quenching of the excitons.<sup>Error! Bookmark not defined.</sup> More importantly, the emitters have low LUMO energy levels and good electron mobilities, which improve their EI and ET ability, respectively, and finally enhance the charge balance of the devices.

**Table 3.** EL performances of the devices D1 and D2.

Device	$V_{\text{turn-on}}^a$ (V)	$L_{\text{max}}^b$ ( $\text{cd m}^{-2}$ )	$\eta_{c,max}^c$ ( $\text{cd A}^{-1}$ )	$\eta_{c, L10000}^d$ ( $\text{cd A}^{-1}$ )	$\text{EQE}_{max}^e$ (%)	$\eta_{p,max}^f$ ( $\text{lm W}^{-1}$ )	$\text{CIE}^g(x, y)$
D1 (8 wt%)	3.6	44885	69.7	65.8	21.7%	41.8	(0.22, 0.59)
D2 (8 wt%)	3.8	92297	91.4	87.7	25.5%	59.4	(0.25, 0.64)

<sup>a</sup>The voltage at a luminance of 1  $\text{cd m}^{-2}$ . <sup>b</sup>Maximum luminance. <sup>c</sup>Maximum current efficiency. <sup>d</sup>The current efficiency at a luminance of 10000  $\text{cd m}^{-2}$ .

<sup>e</sup>Maximum external quantum efficiency. <sup>f</sup>Maximum power efficiency. <sup>g</sup>Calculated at 6 V.

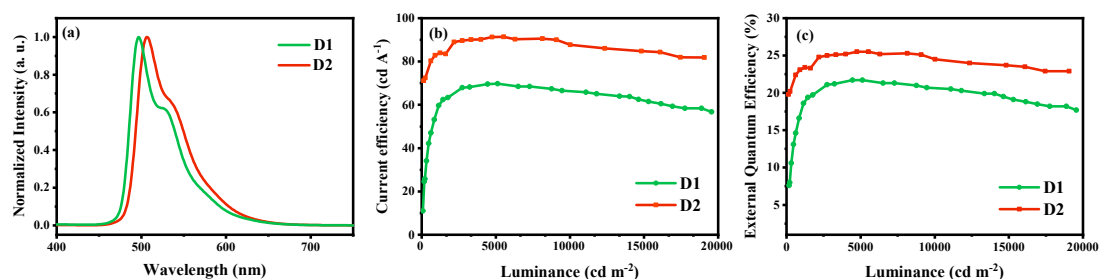


**Fig. 5** Characteristics of device D1 and D2: (a) electroluminescence spectra (6 V); (b) current-efficiency-luminance ( $\eta_{c-L}$ ) curves; (c) external quantum efficiency-luminance ( $\text{EQE-L}$ ) curves.

## Conclusions

In summary, the effect of pyridine sulfonic acid ( $\text{PySO}_3$ ) as ancillary ligands in Ir(III) complexes for high-efficient OLEDs was studied in details. Two green-emitting Ir(III) complexes Ir1 and Ir2 with emission peaks at 496 and 504 nm, respectively, exhibit good thermal stability. Besides, the introduction of

strong polar  $\text{PySO}_3$  moiety lowers down the LUMO energy levels and improves the electron mobility of emitters which facilitates the electron injection possess and enhances the balance of carries. Therefore, device with double light-emitting layers using Ir2 as emitter obtains excellent performances with a  $L_{\text{max}}$  above 92000  $\text{cd m}^{-2}$ , a  $\eta_{c,max}$  of 91.4  $\text{cd A}^{-1}$  and an  $\text{EQE}_{max}$

of 25.5%. Moreover, the EQE still remains 22.9% even at the luminance of 20000 cd m<sup>-2</sup> and the EQE curves decrease slowly as the luminance increases exhibiting an extremely low efficiency roll-off, which is rare among the reported green-emitting OLEDs as well.

## Conflicts of interest

There are no conflicts to declare.

## Acknowledgements

This work was supported by the National Natural Science Foundation of China (51773088).

## Notes and references

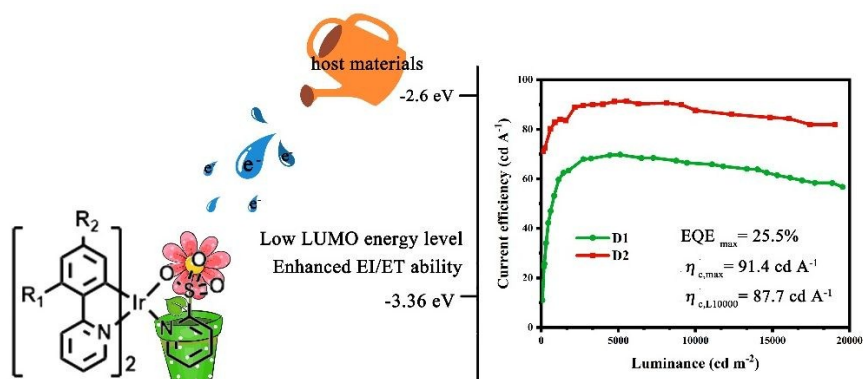
<sup>1</sup>State Key Laboratory of Coordination Chemistry, Collaborative Innovation Center of Advanced Microstructures, Jiangsu Key Laboratory of Advanced Organic Materials, School of Chemistry and Chemical Engineering, Nanjing University, Nanjing 210093, P. R. China, E-mail: yxzheng@nju.edu.cn

<sup>2</sup>MaAnShan High-Tech Research Institute of Nanjing University, MaAnShan, 238200, P. R. China

†Electronic Supplementary Information (ESI) available: Details of measurements. Synthetic method for the complexes and their NMR spectra, detailed crystallographic data and theoretic calculation data, TGA, CV and lifetime curves. EL data including electron mobility of Alq<sub>3</sub>, J-V-L and η<sub>p</sub>-L curves of device D1 and D2.

- M. A. Baldo, S. Lamansky, P. E. Burrows, M. E. Thompson and S. R. Forrest, *Appl. Phys. Lett.*, 1999, **75**, 4.
- C. W. Tang and S. A. VanSlyke, *Appl. Phys. Lett.*, 1987, **51**, 913.
- M. A. Baldo, M. E. Thompson and S. R. Forrest, *Nature*, 2000, **403**, 750.
- Q. Zhang, D. Tsang, H. Kuwabara, Y. Hatae, B. Li, T. Takahashi, S. Y. Lee, T. Yasuda and C. Adachi, *Adv. Mater.*, 2015, **27**, 2096.
- X. Yang, X. Xu, J. Dang, G. Zhou, C. L. Ho and W. Y. Wong, *Inorg. Chem.*, 2016, **55**, 1720.
- J. B. Kim, S. H. Han, K. Yang, S. K. Kwon, J. J. Kim and Y. H. Kim, *Chem. Commun.*, 2014, **51**, 58.
- D. D. Ma, C. Zhang, R. H. Liu, Y. Qiu and L. Duan, *Chem. Eur. J.*, 2018, **24**, 5574.
- V. G. Sree, A. Maheshwaran, H. Kim, H. Y. Park, Y. Kim, J. C. Lee, M. Song and S. H. Jin, *Adv. Funct. Mater.*, 2018, **28**, 1804714.
- D. Escudero and D. Jacquemin, *Dalton Trans.*, 2015, **44**, 8346.
- C. Murawski, K. Leo and M. Gather, *Adv. Mater.*, 2013, **25**, 6801.
- A. Chaskar, H. Chen, and K. Wong, *Adv. Mater.*, 2011, **23**, 3876.
- Z. Gao, M. Luo, X. Sun, H. Tam, M. Wong, B. Mi, P. Xia, K. Cheah and C. Chen, *Adv. Mater.*, 2009, **21**, 688.
- H. Benjamin, M. A. Fox, A. S. Batsanov, H. A. Al-Attar, C. Li, Z. Ren, A. P. Monkman and M. R. Bryce, *Dalton Trans.*, 2017, **46**, 10996.
- C. Fan, Y. Li, C. Yang, H. Wu, J. Qin and Y. Cao, *Chem. Mater.*, 2012, **24**, 4581.
- W. Zhang, Y. Luo, Y. Xu, W. Li and W. Shen, *ChemPhysChem*, 2016, **17**, 4149.
- Y. Hisamatsu and S. Aoki, *Eur. J. Inorg. Chem.*, 2011, **2011**, 5360.
- G. Zhou, C. L. Ho, W. Y. Wong, Q. Wang, D. Ma, L. Wang, Z. Lin, T. B. Marder and A. Beeby, *Adv. Funct. Mater.*, 2008, **18**, 499.
- G. Zhou, X. Yang, W. Y. Wong, Q. Wang, S. Suo, D. Ma, J. Feng and L. Wang, *ChemPhysChem*, 2011, **12**, 2836.
- J. Zhao, Y. Yu, X. Yang, X. Yan, H. Zhang, X. Xu, G. Zhou, Z. Wu, Y. Ren and W. Y. Wong, *ACS Appl. Mater. Interfaces*, 2015, **7**, 24703.
- J. M. Koelewijn, M. Lutz, W. I. Dzik, R. J. Detz and J. N. H. Reek, *ACS Catal.*, 2016, **6**, 3418.
- M. Murata, M. Kojima, A. Hioki, M. Miyagawa, M. Hirotsu, K. Nakajima, M. Kita, S. Kashino and Y. Yoshikawa, *Coord. Chem. Rev.*, 1998, **174**, 109.
- Y. Zheng, Q. X. Zhou, Y. Y. Zhang, C. Li, Y. J. Hou and X. S. Wang, *Dalton Trans.*, 2016, **45**, 2897.
- S. Hu, K. H. He, M. H. Zeng, H. H. Zou and Y. M. Jiang, *Inorg. Chem.*, 2008, **47**, 5218.
- T. S. Lobana, I. Kinoshita, K. Kimura, T. Nishioka, D. Shiomi and K. Isobe, *Eur. J. Inorg. Chem.*, 2004, **2004**, 356.
- E. Baranoff, I. Jung, R. Scopelliti, E. Solari, M. Grätzel and M. K. Nazeeruddin, *Dalton Trans.*, 2011, **40**, 6860.
- R. Davidson, Y. T. Hsu, G. C. Griffiths, C. Li, D. Yufit, R. Pal and A. Beeby, *Inorg. Chem.*, 2018, **57**, 14450.
- E. Arunan, G. R. Desiraju, R. A. Klein, J. Sadlej, S. Scheiner, I. Alkorta, D. C. Clary, R. H. Crabtree, J. J. Dannenberg, P. Hobza, H. G. Kjaergaard, A. C. Legon, B. Mennucci and D. J. Nesbitt, *Pure Appl. Chem.*, 2011, **83**, 1619.
- D. O'Reilly, R. S. Stein, M. B. Patrasco, S. K. Jana, J. Kurian, N. Moitessier and M. J. Damha, *Chem. Eur. J.*, 2018, **24**, 16432.
- P. A. Champagne, J. Desroches and J. F. Paquin, *Synthesis*, 2014, **47**, 306.
- C. Liu, X. Lv, Y. Xing and J. Qiu, *J. Mater. Chem. C*, 2015, **3**, 8010.
- Q. L. Xu, C. C. Wang, T. Y. Li, M. Y. Teng, S. Zhang, Y. M. Jing, X. Yang, W. N. Li, C. Lin, Y. X. Zheng, J. L. Zuo and X. Z. You, *Inorg. Chem.*, 2013, **52**, 4916.
- K. P. S. Zanoni, B. K. Kariyazaki, A. Ito, M. K. Brennaman, T. J. Meyer and N. Y. Iha, *Inorg. Chem.*, 2014, **53**, 4089.
- X. Liang, F. Zhang, Z. P. Yan, Z. G. Wu, Y. Zheng, G. Cheng, Y. Wang, J. L. Zuo, Y. Pan and C. M. Che, *ACS Appl. Mater. Interfaces*, 2019, **11**, 7184.
- B. W. D'Andrade, S. Datta, S. R. Forrest, P. Djurovich, E. Polikarpov and M. E. Thompson, *Org. Electron.*, 2005, **6**, 11.
- B. Xu, L. Chen, X. Liu, H. Zhou, H. Xu, X. Fang, and Y. Wang, *Appl. Phys. Lett.*, 2008, **92**, 103305.
- H. H. Fong, K. C. Lun and S. K. So, *Chem. Phys. Lett.*, 2002, **353**, 407.
- Z. G. Wu, Y. X. Zheng, L. Zhou, Y. Wang and Y. Pan, *Org. Electron.*, 2017, **42**, 141.
- B. Xu, L. Chen, X. Liu, H. Zhou, H. Xu, X. Fang and Y. Wang, *Appl. Phys. Lett.*, 2008, **92**, 103305.
- P. M. Borsenberger and H. Bässler, *Phys. Status Solidi. B*, 1992, **170**, 291.
- S. Su, T. Chiba, T. Takeda and J. Kido, *Adv. Mater.*, 2008, **20**, 2125.
- A. Chaskar, H. Chen and K. Wong, *Adv. Mater.*, 2011, **23**, 3876.
- H. Kim, H. Park, J. H. Jang, W. Song, I. Jung, J. Lee, and D.-H. Hwang, *Dyes and Pigm.*, 2018, **156**, 395.

- 43 B. Tong, H. Wang, M. Chen, S. Zhou, Y. Hu, Q. Zhang, G. He, L. Fu, H. Shi, L. Jin, and H. Zhou, *Dalton Trans.*, 2018, **47**, 12243.
- 44 Z. Chen, L. Wang, C. L. Ho, S. Chen, S. Suramitr, A. Plucksacholatan, N. Zhu, S. Hannongbua, and W. Y. Wong, *Adv. Opt. Mater.*, 2018, **6**, 1800824.
- 45 X. Ma, J. Liang, F. Bai, K. Ye, J. Xu, D. Zhu, and M. R. Bryce, *Eur. J. Inorg. Chem.*, 2018, **2018**, 4614.
- 46 X. Ning, C. Zhao, B. Jiang, S. Gong, D. Ma, and C. Yang, *Dyes and Pigm.*, 2019, **164**, 206.
- 47 C. Zhang, D. Ma, R. Liu, and L. Duan, *J. Mater. Chem. C*, 2019, **7**, 3503.
- 48 X. Zhou, D. S. Qin, M. Pfeiffer, J. Blochwitz-Nimoth, A. Werner, J. Drechsel, B. Maening and K. Leo, *Appl. Phys. Lett.*, 2002, **81**, 4070.



A pyridine sulfonic acid has been developed for green-emitting iridium(III) compounds, which exhibit an EQE<sub>max</sub> of 25.5% with extremely low efficiency roll-off, as well as the EQE still remains 22.9% at 20000 cd m<sup>-2</sup>.